

Article

The Low Expression of Fc-Gamma Receptor III (CD16) and High Expression of Fc-Gamma Receptor I (CD64) on Neutrophil Granulocytes Mark Severe COVID-19 Pneumonia

Joerg Hoffmann *^{ORCID}, Rojin Etati, Cornelia Brendel ^{ORCID}, Andreas Neubauer ^{ORCID} and Elisabeth Mack ^{ORCID}

Department of Hematology, Oncology and Immunology, University Hospital Giessen and Marburg, Philipps University Marburg, Baldingerstrasse, D-35043 Marburg, Germany

* Correspondence: hoffmanx@staff.uni-marburg.de

Abstract: Hyperinflammation through neutrophil granulocytes contributes to disease severity in COVID-19 pneumonia and promotes acute lung failure. Understanding the mechanisms of the dysregulations within the myeloid cell compartment may help to improve therapies for severe COVID-19 infection. Here, we investigated the immunopathological characteristics of circulating neutrophil granulocytes and monocytes in 16 patients with COVID-19 pneumonia by multiparameter flow cytometry in comparison to 9 patients with pulmonary infiltrates but without COVID-19. We correlated the immunophenotypes with the scores of the severity-of-disease classification system, APACHE-II. We found that the mean fluorescence intensity (MFI) of CD15, which is important for the transendothelial migration, was significantly reduced in the patients with COVID-19 (difference \pm SD; 295.70 ± 117.50 MFI; $p = 0.02$). In addition, the granularity was significantly lower in the neutrophil granulocytes of patients with COVID-19 (difference \pm SD; 1.11 ± 0.43 side-scatter ratio; $p = 0.02$). Moreover, the Fc-gamma receptor III (CD16) and Fc-gamma receptor I (CD64) on the neutrophil granulocytes were expressed discordantly with COVID-19 severity. CD16 correlated as inversely proportional ($\rho = (-)0.72$; 95% CI $(-)0.92$ – $(-)0.23$; $p = 0.01$) and CD64 as proportional ($\rho = 0.76$; 95% CI 0.31 – 0.93 ; $p = 0.01$) with the APACHE-II scores of the patients. We conclude that the deviant expression of the Fc-gamma receptors might play role in a dysregulated antibody-mediated phagocytosis in severe cases of COVID-19 pneumonia.

Keywords: COVID-19; corona; pneumonia; flow cytometry; CD16; CD64; Fc-gamma receptor



Citation: Hoffmann, J.; Etati, R.; Brendel, C.; Neubauer, A.; Mack, E. The Low Expression of Fc-Gamma Receptor III (CD16) and High Expression of Fc-Gamma Receptor I (CD64) on Neutrophil Granulocytes Mark Severe COVID-19 Pneumonia. *Diagnostics* **2022**, *12*, 2010. <https://doi.org/10.3390/diagnostics12082010>

Academic Editor: Aw Tar-Choon

Received: 3 July 2022

Accepted: 17 August 2022

Published: 19 August 2022

Publisher's Note: MDPI stays neutral with regard to jurisdictional claims in published maps and institutional affiliations.



Copyright: © 2022 by the authors. Licensee MDPI, Basel, Switzerland. This article is an open access article distributed under the terms and conditions of the Creative Commons Attribution (CC BY) license (<https://creativecommons.org/licenses/by/4.0/>).

1. Introduction

The severe acute respiratory syndrome coronavirus 2 (SARS-CoV-2), the cause of coronavirus disease 2019 (COVID-19), appeared in December 2019 in Wuhan, China [1]. The fight against the COVID-19 pandemic and its consequences on health care systems and societies are issues of worldwide importance. A total of 574 million confirmed COVID-19 cases and 6.3 million deaths had reported globally by the end of July 2022 [2]. In the U.S., between January and May 2020, about 14% of all COVID-19 cases required hospitalization, 2% were admitted to an intensive care unit (ICU), and 5% resulted in death [3]. The outbreak of the Omicron variant in November 2021 resulted in decreased death rates (4.5% vs. 21.3%) and ICU admissions (1% vs. 4.3%) compared to the previous waves in South Africa [4].

COVID-19 can result in acute respiratory distress syndrome (ARDS) with rapidly progressive lung failure [5,6]. ARDS is a complication of the COVID-19 infection, with high morbidity and mortality. In particular, patients of older ages or with comorbidities are at an increased risk, and more often experience a difficult course, of disease [7–10]. A dysregulated immune response with cytokine-induced hyperinflammation contributes to the morbidity and mortality of COVID-19 [11–13]. Several studies have demonstrated

favorable outcomes with the use of immune response modifiers in patients with severe COVID-19 infections [14–19].

A high neutrophils/lymphocyte ratio helps to predict severe COVID-19 [14,20,21]. After neutrophil granulocytes, monocytes are the second most abundant group of myeloid cells in the peripheral blood. Monocytes can be separated into at least three different subsets: the CD16 (Fc-gamma receptor III)-negative classical subset and the intermediate and non-classical CD16-positive subsets [22–25]. The CD16-positive subsets are more involved in antigen presentation and Fc-gamma-mediated phagocytosis than the classical monocytes [26,27]. In a comprehensive analysis, Schulte-Schrepping et al. described abundant alterations in the myeloid cell compartment associated with COVID-19, such as the predominance of inflammatory monocytes in mild cases of the disease, whereas dysfunctional monocytes occurred primarily in severe COVID-19 [28]. Important questions concerning the role of neutrophil granulocytes and monocytes in hyperinflammation and their therapeutic implications in COVID-19 remain to be elucidated.

The main objective of this study was to identify characteristics in the immunophenotype of the neutrophil granulocytes and monocytes that are distinctive of a COVID-19 infection and indicate a severe course of the disease. This discovery could aid in the clinical assessment of COVID-19 patients and improve our understanding of the role of immunopathological dysregulation in COVID-19. Therefore, we investigated the expression of cell surface proteins with key functions (i.e., adhesion, migration, extravasation, and phagocytosis) in the immune response of the neutrophil granulocytes and monocytes in patients with COVID-19 pneumonia and compared the findings to patients with pulmonary infiltrates but without COVID-19.

2. Materials and Methods

2.1. Patients

This study was performed at the beginning of the first wave of the COVID-19 pandemic in Germany, between March and May 2020, at a single academic center (University Hospital Marburg). A total of 30 patients with clinical symptoms of respiratory infection compatible with COVID-19 were enrolled. Peripheral blood samples were collected after written informed consent was obtained. The study was conducted according to the guidelines of the local ethics committee (Vote 57/20) and the Declaration of Helsinki. Pulmonary infiltrates identified on the CT scan were mandatory for inclusion in the final analysis. Patients were tested for SARS-CoV-2 infection with combined E- and S-specific PCR (RealStar[®] SARS-CoV-2 RT-PCR Kit, Altona Diagnostics, Hamburg, Germany) using a nasopharyngeal swab and separated into a COVID-19-positive group and a control group.

We measured the expression of the cell surface proteins with respect to their adhesion, migration, extravasation (CD15, CD38, and CD11b), (antibody-mediated) phagocytosis and apoptosis (CD33, CD36, CD16, CD64, and CD13), and antigen-presentation (HLA-DR) via multiparameter flow cytometry (MPFC) applied to the neutrophil granulocytes and monocytes. In addition, the release of soluble anti-microbial granules (i.e., granularity) was quantified for the neutrophil granulocytes. The monocytes were analyzed for the expression of the pattern recognition receptor CD14, aberrant expression of the cell-to-cell adhesion molecule CD56, and the count of the CD16-positive monocyte subset (non-classical and intermediate). Immunophenotypic characteristics of the granulocytes and monocytes of the patients in intensive care units (ICU) with COVID-19 were aligned with the APACHE-II scores, which are prognostic for morbidity and mortality [29]. The severity of ARDS was assessed using the Horowitz index [30,31]. Other clinical parameters, such as age, number of days in the hospital or ICU, comorbidities (Charlson comorbidity index, CCI), inflammation (C-reactive protein and procalcitonin), and coagulation (d-dimer, thrombocytes, fibrinogen, prothrombin time, activated partial thromboplastin time, and thrombin clotting time) were correlated in relation to the immunophenotypic characteristics.

Sample handling, flow cytometry data acquisition, and analysis.

A total of $2 \times 100 \mu\text{L}$ peripheral blood was transferred into two separate 5 mL polystyrene tubes with fluorescence antibodies in a dried-down layer (DURAClone Technology, Beckman Coulter, Brea, CA, USA) and incubated for 15 min at room temperature. The following antibody combinations were used for the immunological studies:

Tube 1: CD15 FITC (clone 80H5), CD33 PE (clone D3HL60.251), CD13 ECD (clone SJ1D1), CD117 PC 5.5 (clone 104D2D1), CD34 PC7 (clone 581), CD10 APC (clone ALB1), CD16 APC-AF700 (clone 3G8), CD11b APC-AF750 (clone BEAR1), HLA-DR Pacific blue (clone IMMU-357), and CD45 Krome orange (clone J33).

Tube 2: CD7 FITC (clone 8H8.1), CD19 PE (clone J3.119), CD38 ECD (clone LS198-4-3), CD56 PC5.5 (clone N901 (NKH-1)), CD34 PC7 (clone 581), CD10 APC (clone ALB1), CD14 APC-AF700 (clone RMO52), CD64 APC-AF750 (clone 22), CD36 Pacific blue (clone FA6.152), and CD45 Krome orange (clone J33) (all from Beckman Coulter).

After antibody staining, red cells were lysed in 2 mL Versalyse (Beckman Coulter) for 10 min, washed with 3 mL phosphate-buffered saline (PBS Biochrom, Berlin, Germany), and centrifuged with $300 \times g$ for 5 min. The cell pellet was resuspended in 500 μL PBS and measured on a Navios flow cytometer (Beckman Coulter). In total, up to 1×10^5 cells were acquired. The flow cytometry analysis and gating were performed with Kaluza vs. 2.1. (Beckman Coulter). Debris, red cells, thrombocyte aggregates were excluded via side-scatter (SSC), forward-scatter (FSC), and the pan-leucocyte antigen CD45. The lymphocytes, monocytes, and granulocytes were pre-gated via the two-dimensional SSC/CD45 plot. Mature neutrophil granulocytes were selected in the CD16/CD13 plot to exclude the eosinophils (CD16-negative) and immature granulocytes/myelocytes (CD13 dim). The monocytes were selected in the CD36/CD14 plot. The relative mean fluorescence intensity was determined using the ratio of the geometric mean fluorescence of the neutrophil granulocytes or monocytes and the geometric mean fluorescence of the negative population of the lymphocytes. The granularity was measured in each sample using the ratio of SSC neutrophil granulocytes/SSC lymphocytes (SSC ratio).

2.2. Statistics

The charts and statistics were compiled on Excel 2016 (Microsoft Corporation, Redmond, WA, USA) and GraphPad Prism[®] Version 5.00 (GraphPad Software, San Diego, CA, USA). The relative MFI from CD15, CD38, CD11b, CD33, CD36, CD16, CD64, CD13, HLA-DR, CD14, and CD56, and granularity and percentages/counts for CD16-positive monocytes, were compared between patients with COVID-19 and without COVID-19 using the Mann–Whitney U test. Significantly different antigens ($p < 0.05$) were analyzed based on receiver operating characteristic (ROC) curves for the binary classification. Immunophenotypic characteristics were correlated with the clinical parameters using Spearman's rank correlation coefficient. Results of the correlation coefficient ρ were depicted in a correlation matrix (heat map).

3. Results

3.1. Study Population and Patient Characteristics

In total, 30 patients were hospitalized with suspected COVID-19 and enrolled in the study. CT scans revealed pulmonary infiltrates in 26 patients. The MPFC was performed without measurement errors in 25 patients, who were included in the final analysis of the immunophenotypes of myeloid cells (Figure 1).

The median age of the patients was 67 years (range 23–88 years) and 19% were female. The median duration of hospitalization was 28 days (range 7–67 days) and patients in the ICU received intensive care for a median of 19 days (range 2–49 days). A total of 21/25 (84%) patients were discharged from hospital and 4/25 (16%) patients died during hospitalization. At baseline, 16/25 (64%) patients had a positive SARS-CoV-2 PCR result and 18/25 (72%) were admitted to the ICU. In the ICU subgroup, 12 patients were positive for SARS-CoV-2 and 4 patients were negative, and in the non-ICU group, 4 patients were positive and 3 were negative for SARS-CoV-2. All nine patients who were negative for

SARS-CoV-2 had an atypical form of pneumonia, but no causative pathogen could be found. Procalcitonin, as a marker of a bacterial infection, was elevated in four out of nine (44%) patients without SARS-CoV-2. Further patient characteristics are denoted in Table 1.

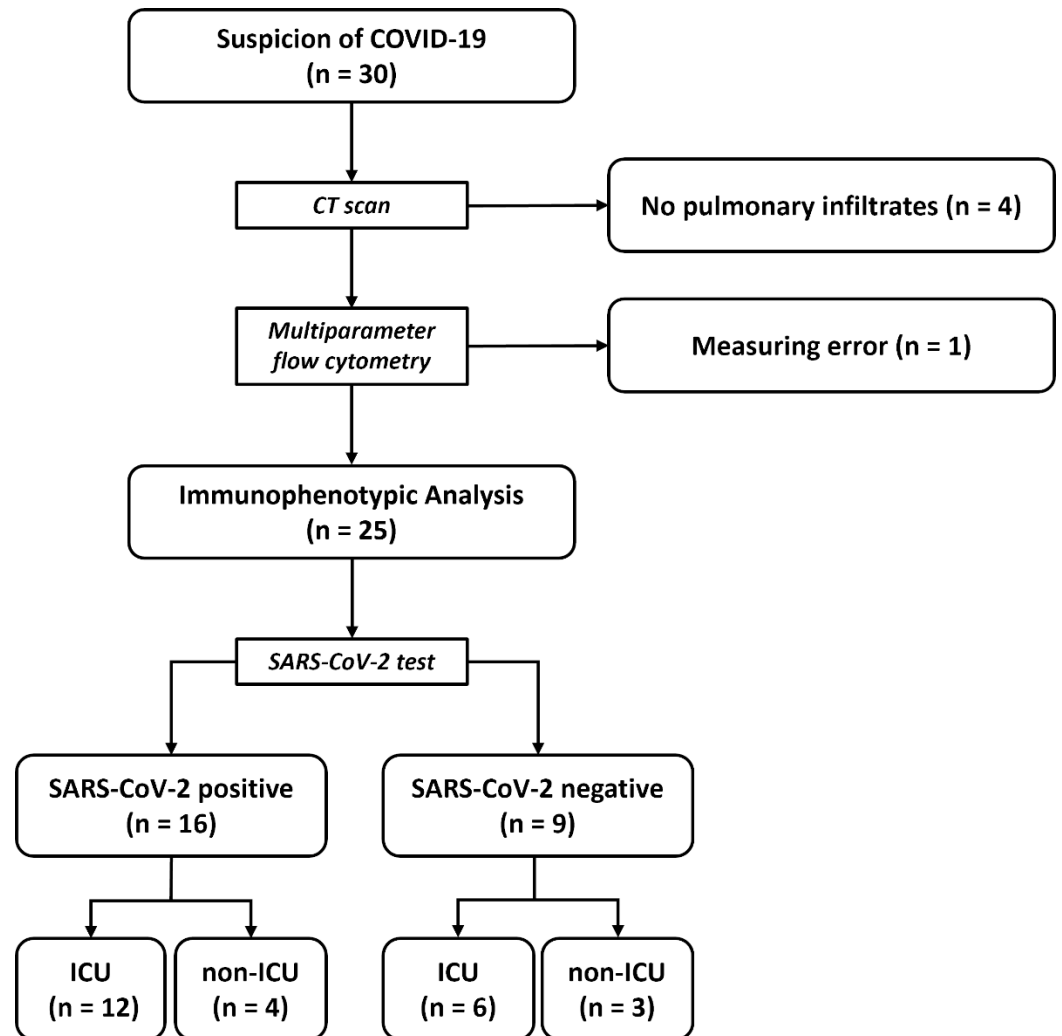


Figure 1. Study population and workflow. Abbreviations: *n* = number; ICU = intensive care unit, SARS-CoV-2 = severe acute respiratory syndrome coronavirus 2.

Table 1. Patient characteristics.

Characteristic	COVID-19 Positive (<i>n</i> = 16)	COVID-19 Negative (<i>n</i> = 9)
Median age (range)—years	66.5 (23–82)	70 (28–88)
Male sex—no. (%)	13 (81%)	5 (56%)
Female sex—no. (%)	3 (19%)	4 (44%)
Underlying Health Condition—No./Total No. (%)		
Diabetes	6 (38%)	1 (11%)
Hypertension	11 (69%)	5 (56%)
Obesity (BMI ≥ 30)	4 (25%)	2 (22%)
Hyperlipidemia	3 (19%)	0 (0%)
Chronic heart disease	5 (31%)	1 (11%)
Cardiovascular disease	3 (19%)	4 (44%)
Respiratory disease	1 (6%)	3 (33%)
Chronic kidney disease	1 (6%)	3 (33%)

Table 1. Cont.

Characteristic	COVID-19 Positive (<i>n</i> = 16)	COVID-19 Negative (<i>n</i> = 9)
Cancer	3 (19%)	3 (33%)
Immunosuppression	3 (19%)	1 (11%)
Chronic liver disease	2 (13%)	1 (11%)
Charlson Comorbidity Index -/median (range)	4 (1–7)	5 (0–11)
Complications—No./Total No. (%)		
Acute respiratory distress syndrome	11 (69%)	4 (44%)
Non-invasive ventilation	0 (0%)	2 (22%)
Invasive mechanical ventilation	11 (69%)	4 (44%)
Acute kidney failure	8 (50%)	2 (22%)
Thromboembolic events	3 (19%)	0 (0%)
ICU	12 (75%)	6 (67%)
Death	3 (19%)	1 (11%)

3.2. Immunological Differences between SARS-CoV-2-Positive and SARS-CoV-2-Negative Patients

The neutrophil granulocytes in patients with a positive SARS-CoV-2 test (*n* = 16) had a significantly reduced CD15 expression (difference \pm SD; 295.70 ± 117.50 MFI; *p* = 0.02) and reduced SSC ratio (i.e., granularity; difference \pm SD; 1.11 ± 0.43 SSC-Ratio; *p* = 0.02) than patients with a negative SARS-CoV-2 test (*n* = 9) in the Mann–Whitney test (Figure 2A,B).

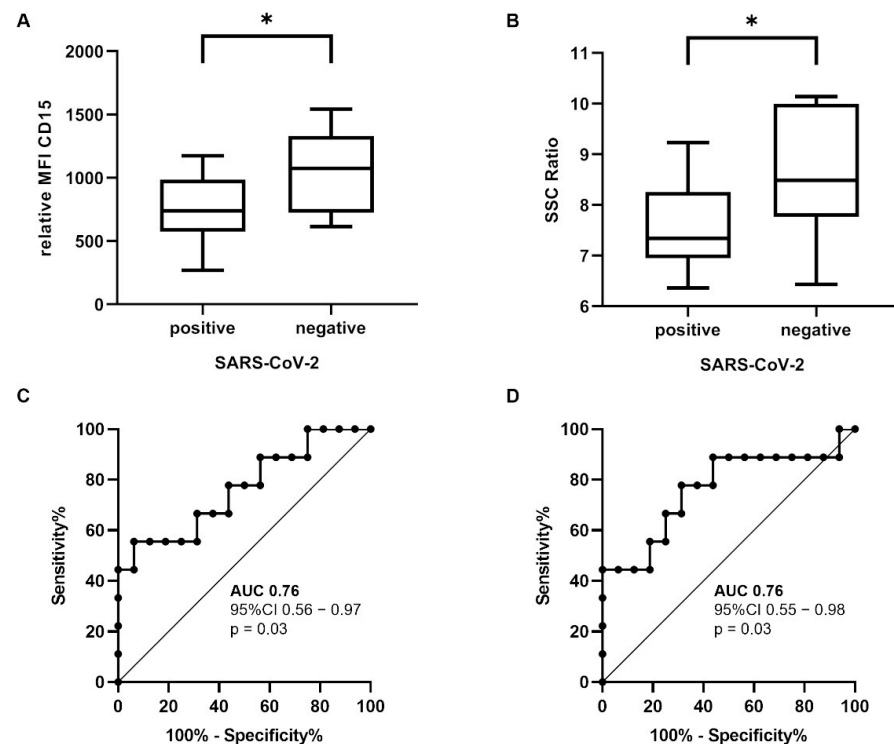


Figure 2. Immunophenotypic differences of the circulating neutrophil granulocytes. CD15 (A) and SSC ratio (B) were significantly reduced in patients with SARS-CoV-2 infection (difference \pm SD; 295.70 ± 117.50 MFI; *p* = 0.02 and 1.11 ± 0.43 SSC ratio; *p* = 0.02). ROC curves showed an AUC of 0.76 for the CD15 (C) and SSC ratio (D). Mann–Whitney U test * *p* < 0.05 (abbreviations: *n* = number; MFI = mean fluorescence intensity; SSC = side-scatter; SARS-CoV-2 = severe acute respiratory syndrome coronavirus 2; AUC = area under curve; CI = confidence interval; ROC = receiver operating characteristic).

We performed an ROC analysis to examine whether CD15 and SSC are useful as binary classifiers for distinguishing between SARS-CoV-2-positive and SARS-CoV-2-negative patients (Figure 2C,D). CD15 had an area under curve (AUC) of 0.76 (95% CI 0.56–0.97; $p = 0.03$) and SSC had an AUC of 0.76 (95% CI 0.55–0.98, $p = 0.03$). This means that the CD15 and SSC of neutrophil granulocytes could discriminate between SARS-CoV-2-positive and SARS-CoV-2-negative patients in 76% of the cases.

In the monocyte compartment, the expression of CD15 did not distinguish between SARS-CoV-2-positive and SARS-CoV-2-negative patients ($p = 0.96$). However, the CD14 expression was significantly diminished in patients with SARS-CoV-2 infection compared to patients without the infection in the Mann–Whitney U test (difference \pm SD; 405.90 ± 177.40 MFI; $p = 0.03$), whereas the counts of the CD16 + monocytes were significantly higher (difference \pm SD; 0.07 ± 0.03 per nl; $p = 0.01$) (Figure 3A,B). The ROC curves showed an AUC of 0.76 (95% CI 0.55–0.98, $p = 0.03$) for the CD14 expression and an AUC of 0.81 (95% CI 0.64–0.98, $p = 0.01$) (Figure 3C,D) for the CD16 + monocyte count. Together, our findings indicate that the CD16 + monocyte count is the most robust diagnostic parameter for identifying a SARS-CoV-2 infection in the myeloid cell compartment.

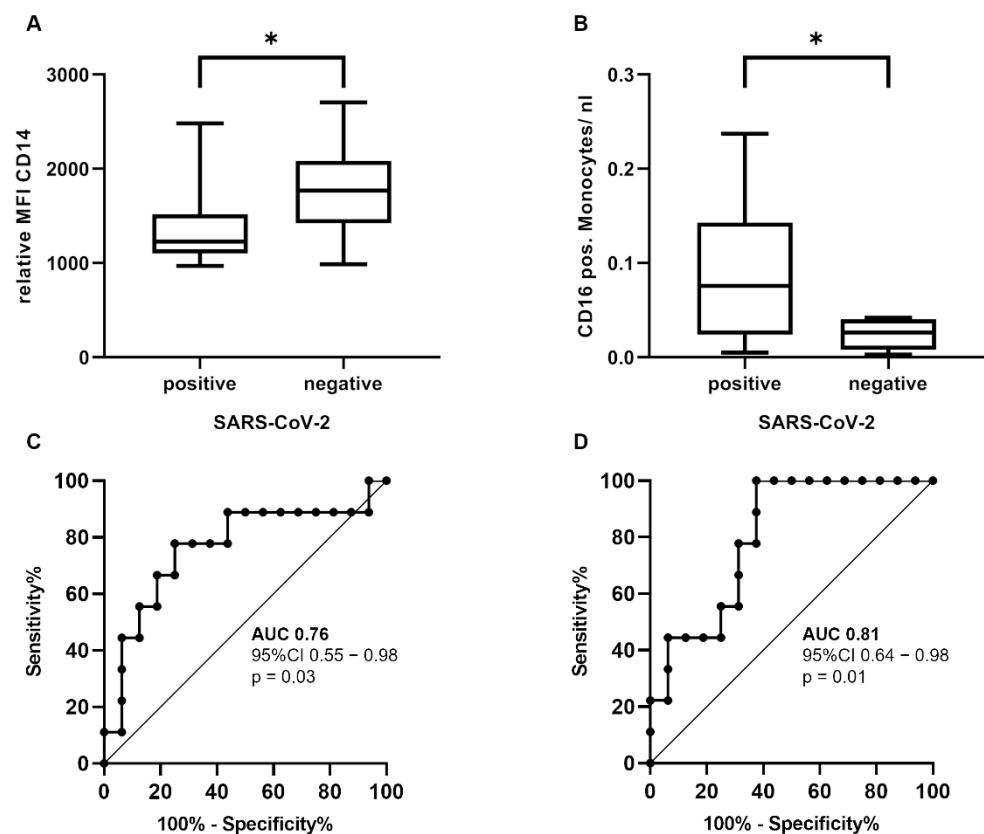


Figure 3. Immunophenotypic differences of the circulating monocytes. The CD14 expression (A) was significantly reduced (difference \pm SD; 405.90 ± 177.40 MFI; $p = 0.03$) and the CD16 + monocyte count (B) significantly increased (difference \pm SD; 0.07 ± 0.03 per nl; $p = 0.01$) in patients with SARS-CoV-2 infection. ROC curves showed an AUC of 0.76 for CD14 (C) and an AUC of 0.81 for the CD16 + monocyte count (D). Mann–Whitney U test with $* p < 0.05$ (abbreviations: n = number; MFI = mean fluorescence intensity; SSC = side-scatter; SARS-CoV-2 = severe acute respiratory syndrome coronavirus 2, AUC = area under curve; CI = confidence interval; ROC = receiver operating characteristic).

3.3. Immunological Characteristics of Severe COVID-19 Infection

Next, we turn to the immunological differences between the patients with or without SARS-CoV-2 infection. We searched for markers of a severe course of COVID-19 infection

within the patients who were admitted to an ICU ($n = 12$). The disease severity was assessed based on the APACHE-II score and Horowitz- index, which are related to the morbidity and mortality of ICU patients and the degree of ARDS, respectively. In addition, immunological characteristics were correlated with other clinical parameters, such as age, number of days in the hospital or ICU, the Charlson comorbidity index, inflammation (C-reactive protein and procalcitonin), coagulation (d-dimer, thrombocytes, fibrinogen, prothrombin time, activated partial thromboplastin time, and thrombin clotting time). The Spearman’s correlation matrix results for the immunophenotypic characteristics of the neutrophil granulocytes are depicted in Figure 4, and those for the monocytes are depicted in Figure 5. Severe COVID-19 infection was correlated with a low CD16 expression ($r = (-) 0.72$; 95% CI $(-)0.92-(-)0.23$; $p = 0.01$) and high CD64 expression ($r = 0.76$; 95% CI $0.31-0.93$; $p = 0.01$) in the neutrophil granulocytes, and ARDS was correlated with CD36 expression ($r = 0.66$, 95% CI $0.07-0.91$; $p = 0.03$).

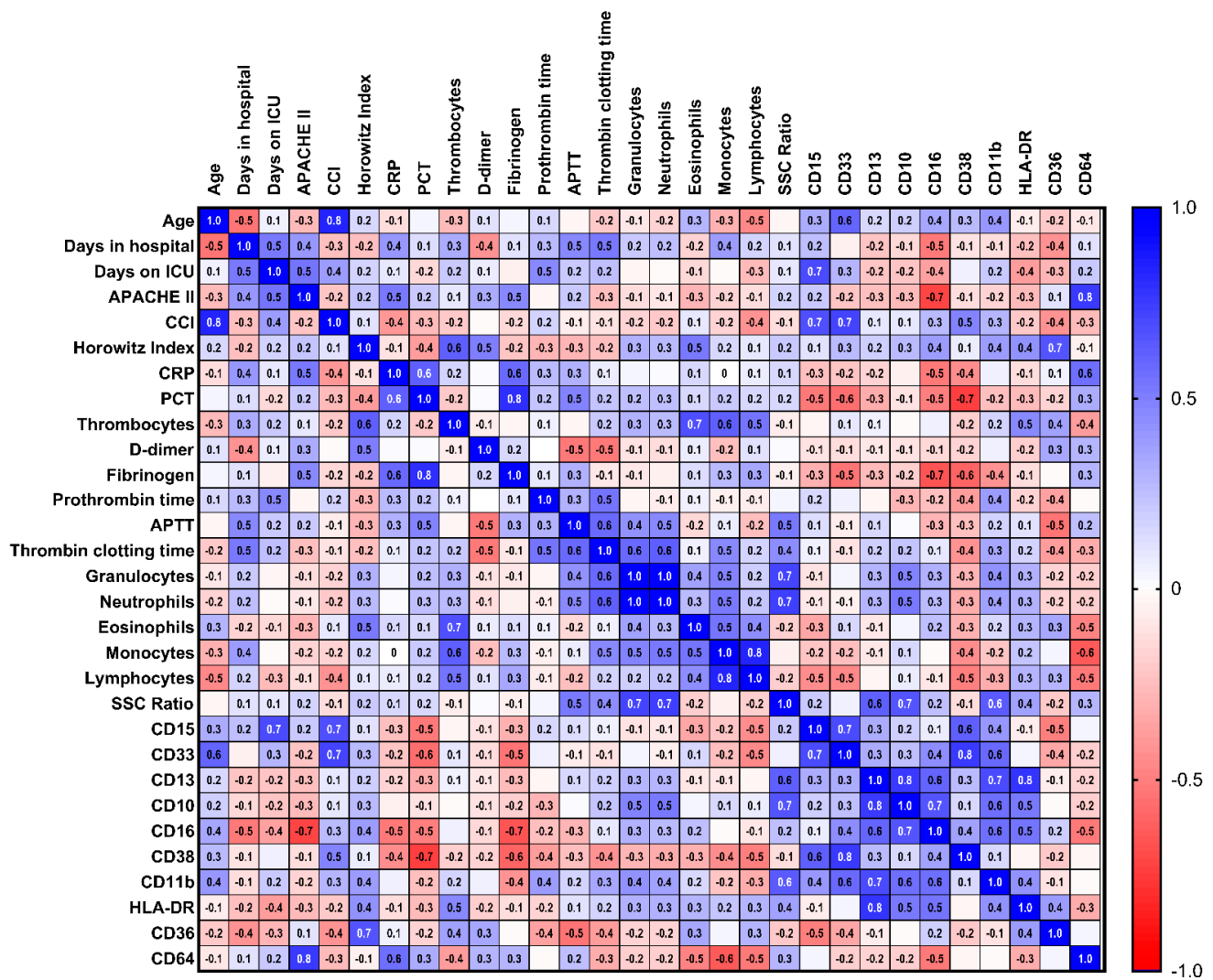


Figure 4. Correlation matrix of the neutrophil granulocytes and clinical parameters. Correlation matrix (heat map) of the immunophenotypic characteristics of the neutrophil granulocytes and clinical parameters of patients with COVID-19 in the ICU ($n = 12$). Spearman’s ρ ranks between ± 1.0 (dark blue, dark red), high (inverse) correlation, and ± 0 (white), no correlation (abbreviations: ICU = intensive care unit; $n =$ number; APACHE = acute physiology and chronic health evaluation; CCI = Charlson comorbidity index; CRP = C-reactive protein; PCT = procalcitonin; APTT = activated partial thromboplastin time; SSC = side-scatter).

4. Discussion

In this study, we showed that the circulating neutrophil granulocytes of patients with COVID-19 pneumonia have significantly a lower granularity and expression of CD15, whereas monocytes express decreased levels of CD14. Furthermore, the counts of the monocyte subsets with CD16 expression, which belong to the non-classical and intermediate monocyte categories, were significantly increased in patients with COVID-19. Our results are in line with previous reports that described a dysregulated myeloid cell compartment in cases of severe COVID-19 disease [28,32]. More specifically, Zhou et al. and Silvin et al. identified a higher proportion of the intermediate monocyte subset in COVID-19 disease than in the controls [32,33]. Interestingly, the SARS-CoV-2 S1 protein persists in CD16-positive monocytes after infection and might be associated with post-acute sequelae SARS-CoV-2 infection (long COVID) [34].

The lower expression of CD15 on neutrophils has been reported in patients with COVID-19 [35,36] and was confirmed by our results. CD15 is important for the transendothelial migration of the neutrophils [37,38], and the downregulation of CD15 might be associated with endothelial dysfunction in COVID-19 [39]. Reduced granularity of the neutrophil granulocytes has been described in terms of COVID-19 [40,41], but it is also common in other inflammatory states [42]. Our results gain are bolstered by the consistently selected control group of patients with pulmonary infiltrates but without SARS-CoV-2 infection, who were admitted to hospital within the same period of time. Therefore, our findings shed additional light on the specific immunophenotypes of the myeloid cells in COVID-19 compared to other forms of pneumonia, rather than on a more general difference between a pathologic state and the healthy state of controls.

A low CD16 expression and high CD64 expression on the neutrophil granulocytes was correlated with the severity of the health condition and risk of death (a high APACHE-II score) in patients with COVID-19 in the ICU. This finding is, at first glance, contradictory, because both antigens are Fc-gamma receptors, which bind the IgG molecules within an immune complex. Yet, CD16 is downregulated through proteolysis upon activation and apoptosis [43–45], and CD64 is upregulated through interferon γ (IFN γ) and the granulocyte colony-stimulating factor (G-CSF) in the neutrophil granulocytes [46,47]. CD16 is classified as a low-affinity Fc-gamma receptor III (Fc γ RIII), and CD16b/Fc γ RIIIb is solely expressed on the neutrophil granulocytes [48]. In the case of Fc γ RIIIb ligation to the unspecific Fc region of the antibodies (e.g., IgG) or IgG aggregates, intracellular granules from the neutrophils [49,50] are released. Ankerhold et al. described that soluble circulating IgG immune complexes in SARS-CoV-2 infection, which might contribute to an enhanced CD16b/Fc γ RIIIb activation that results in a “vicious cycle of escalating immunopathology” [51]. This might explain the lower expression of CD16b/Fc γ RIIIb in COVID-19 patients, because the activation of CD16b/Fc γ RIIIb results in the downregulation of CD16b/Fc γ RIIIb [43–45].

CD64 is classified as a high-affinity Fc-gamma receptor I (Fc γ RI) and is normally expressed on the monocytes. It is an indicator of sepsis and might be associated with higher mortality in the ICU [48,48,52–55]. We propose that a low CD16 expression on the neutrophil granulocytes might indicate a severe COVID-19 infection, whereas a high CD64 expression more generally indicates a severe health condition because of its reactivity to IFN γ and G-CSF.

There are limitations to this study. Only patients of the first COVID-19 wave between March and May 2020 in Germany were included. SARS-CoV-2 variants, vaccination statuses, and COVID-19 treatment have changed since then, and these factors might have an impact on the immunopathology of COVID-19 disease. Therefore, our results have to be confirmed in study based on a larger patient cohort and with the new variants of SARS-CoV-2. The disease severity was quantified using the APACHE II score in this study. APACHE II correlates with the hospital death of ICU patients in general [29]. Other disease severity scores might be more specific to patients with COVID-19 pneumonia [56–58].

5. Conclusions

In this study, we showed that neutrophil granulocytes with a low CD15 expression and diminished granularity were characteristic of COVID-19 pneumonia. The severity of COVID-19 infection was correlated with a low expression of CD16 (FcγRIIIb) and high expression of CD64 (FcγRI) on the neutrophil granulocytes. This indicates the important role of Fc-gamma receptors in severe COVID-19 pneumonia.

Author Contributions: Conceptualization, J.H. and E.M.; methodology, R.E.; formal analysis, J.H. and R.E.; investigation R.E.; resources, A.N.; data curation, R.E.; writing—original draft preparation, J.H.; writing—review and editing, C.B., A.N. and E.M.; supervision, C.B, A.N. and E.M.; funding acquisition, A.N. and E.M. All authors have read and agreed to the published version of the manuscript.

Funding: This study was supported in part by the “Europäische Fonds für regionale Entwicklung” (EFRE) (62033243#20007349). This work was supported in part by the José Carreras Leukaemia Foundation under Grant AH 06-01.

Institutional Review Board Statement: The study was conducted in accordance with the Declaration of Helsinki and approved by the Ethics Committee of the Philipps University (Vote 57/20), Approval Date 03-04-2020.

Informed Consent Statement: Informed consent was obtained from all subjects involved in the study.

Data Availability Statement: Not applicable.

Acknowledgments: We thank Andrea Gruen, Ute Niebergall, and Ute Meissauer for their technical assistance. Margrit Gündisch, Sarah Greib, Thomas Tarawneh, Ihab Karim, and Carolin Riemer are acknowledged for their help with sample collection.

Conflicts of Interest: The authors declare no conflict of interest. The funders had no role in the design of the study; in the collection, analysis, or interpretation of the data; in the writing of the manuscript; or in the decision to publish the results.

References

1. Zhu, N.; Zhang, D.; Wang, W.; Li, X.; Yang, B.; Song, J.; Zhao, X.; Huang, B.; Shi, W.; Lu, R.; et al. A Novel Coronavirus from Patients with Pneumonia in China, 2019. *N. Engl. J. Med.* **2020**, *382*, 727–733. [[CrossRef](#)] [[PubMed](#)]
2. Weekly Epidemiological Update on COVID-19—3 August 2022. Available online: <https://www.who.int/publications/m/item/weekly-epidemiological-update-on-covid-19---3-august-2022> (accessed on 8 August 2022).
3. Stokes, E.K.; Zambrano, L.D.; Anderson, K.N.; Marder, E.P.; Raz, K.M.; El Burai Felix, S.; Tie, Y.; Fullerton, K.E. Coronavirus Disease 2019 Case Surveillance—United States, 22 January–30 May 2020. *Morb. Mortal. Wkly. Rep.* **2020**, *69*, 759–765. [[CrossRef](#)] [[PubMed](#)]
4. Abdullah, F.; Myers, J.; Basu, D.; Tintinger, G.; Ueckermann, V.; Mathebula, M.; Ramlall, R.; Spoor, S.; de Villiers, T.; Van der Walt, Z.; et al. Decreased Severity of Disease during the First Global Omicron Variant COVID-19 Outbreak in a Large Hospital in Tshwane, South Africa. *Int. J. Infect. Dis.* **2022**, *116*, 38–42. [[CrossRef](#)]
5. Wölfel, R.; Corman, V.M.; Guggemos, W.; Seilmaier, M.; Zange, S.; Müller, M.A.; Niemeyer, D.; Jones, T.C.; Vollmar, P.; Rothe, C.; et al. Virological Assessment of Hospitalized Patients with COVID-2019. *Nature* **2020**, *581*, 465–469. [[CrossRef](#)]
6. Xu, Z.; Shi, L.; Wang, Y.; Zhang, J.; Huang, L.; Zhang, C.; Liu, S.; Zhao, P.; Liu, H.; Zhu, L.; et al. Pathological Findings of COVID-19 Associated with Acute Respiratory Distress Syndrome. *Lancet Respir. Med.* **2020**, *8*, 420–422. [[CrossRef](#)]
7. Lippi, G.; Mattiuzzi, C.; Sanchis-Gomar, F.; Henry, B.M. Clinical and Demographic Characteristics of Patients Dying from COVID-19 in Italy versus China. *J. Med. Virol.* **2020**, *92*, 1759. [[CrossRef](#)]
8. Lighter, J.; Phillips, M.; Hochman, S.; Sterling, S.; Johnson, D.; Francois, F.; Stachel, A. Obesity in Patients Younger than 60 Years Is a Risk Factor for Covid-19 Hospital Admission. *Clin. Infect. Dis.* **2020**, *71*, 896–897. [[CrossRef](#)]
9. Richardson, S.; Hirsch, J.S.; Narasimhan, M.; Crawford, J.M.; McGinn, T.; Davidson, K.W.; Barnaby, D.P.; Becker, L.B.; Chelico, J.D.; Cohen, S.L.; et al. Presenting Characteristics, Comorbidities, and Outcomes Among 5700 Patients Hospitalized With COVID-19 in the New York City Area. *JAMA* **2020**, *323*, 2052–2059. [[CrossRef](#)]
10. Huang, C.; Wang, Y.; Li, X.; Ren, L.; Zhao, J.; Hu, Y.; Zhang, L.; Fan, G.; Xu, J.; Gu, X.; et al. Clinical Features of Patients Infected with 2019 Novel Coronavirus in Wuhan, China. *Lancet* **2020**, *395*, 497–506. [[CrossRef](#)]
11. Buszko, M.; Nita-Lazar, A.; Park, J.-H.; Schwartzberg, P.L.; Verthelyi, D.; Young, H.A.; Rosenberg, A.S. Lessons Learned: New Insights on the Role of Cytokines in COVID-19. *Nat. Immunol.* **2021**, *22*, 404–411. [[CrossRef](#)]
12. Blanco-Melo, D.; Nilsson-Payant, B.E.; Liu, W.-C.; Uhl, S.; Hoagland, D.; Möller, R.; Jordan, T.X.; Oishi, K.; Panis, M.; Sachs, D.; et al. Imbalanced Host Response to SARS-CoV-2 Drives Development of COVID-19. *Cell* **2020**, *181*, 1036–1045.e9. [[CrossRef](#)] [[PubMed](#)]

13. Lucas, C.; Wong, P.; Klein, J.; Castro, T.B.R.; Silva, J.; Sundaram, M.; Ellingson, M.K.; Mao, T.; Oh, J.E.; Israelow, B.; et al. Longitudinal Analyses Reveal Immunological Misfiring in Severe COVID-19. *Nature* **2020**, *584*, 463–469. [[CrossRef](#)] [[PubMed](#)]
14. Neubauer, A.; Johow, J.; Mack, E.; Burchert, A.; Meyn, D.; Kadlubiec, A.; Torje, I.; Wulf, H.; Vogelmeier, C.F.; Hoyer, J.; et al. The Janus-Kinase Inhibitor Ruxolitinib in SARS-CoV-2 Induced Acute Respiratory Distress Syndrome (ARDS). *Leukemia* **2021**, *35*, 2917–2923. [[CrossRef](#)] [[PubMed](#)]
15. RECOVERY Collaborative Group; Horby, P.; Lim, W.S.; Emberson, J.R.; Mafham, M.; Bell, J.L.; Linsell, L.; Staplin, N.; Brightling, C.; Ustianowski, A.; et al. Dexamethasone in Hospitalized Patients with COVID-19. *N. Engl. J. Med.* **2021**, *384*, 693–704. [[CrossRef](#)]
16. Gupta, S.; Wang, W.; Hayek, S.S.; Chan, L.; Mathews, K.S.; Melamed, M.L.; Brenner, S.K.; Leonberg-Yoo, A.; Schenck, E.J.; Radbel, J.; et al. Association Between Early Treatment With Tocilizumab and Mortality Among Critically Ill Patients With COVID-19. *JAMA Intern. Med.* **2021**, *181*, 41–51. [[CrossRef](#)]
17. Kalil, A.C.; Patterson, T.F.; Mehta, A.K.; Tomashek, K.M.; Wolfe, C.R.; Ghazaryan, V.; Marconi, V.C.; Ruiz-Palacios, G.M.; Hsieh, L.; Kline, S.; et al. Baricitinib plus Remdesivir for Hospitalized Adults with COVID-19. *N. Engl. J. Med.* **2021**, *384*, 795–807. [[CrossRef](#)]
18. Stone, J.H.; Frigault, M.J.; Serling-Boyd, N.J.; Fernandes, A.D.; Harvey, L.; Foulkes, A.S.; Horick, N.K.; Healy, B.C.; Shah, R.; Bensaci, A.M.; et al. Efficacy of Tocilizumab in Patients Hospitalized with COVID-19. *N. Engl. J. Med.* **2020**, *383*, 2333–2344. [[CrossRef](#)]
19. Ghosn, L.; Chaimani, A.; Evrenoglou, T.; Davidson, M.; Graña, C.; Schmucker, C.; Bollig, C.; Henschke, N.; Sguassero, Y.; Nejtgaard, C.H.; et al. Interleukin-6 Blocking Agents for Treating COVID-19: A Living Systematic Review. *Cochrane Database Syst. Rev.* **2021**, *2021*, CD013881. [[CrossRef](#)]
20. Liu, J.; Liu, Y.; Xiang, P.; Pu, L.; Xiong, H.; Li, C.; Zhang, M.; Tan, J.; Xu, Y.; Song, R.; et al. Neutrophil-to-Lymphocyte Ratio Predicts Critical Illness Patients with 2019 Coronavirus Disease in the Early Stage. *J. Transl. Med.* **2020**, *18*, 206. [[CrossRef](#)]
21. Zhang, B.; Zhou, X.; Zhu, C.; Song, Y.; Feng, F.; Qiu, Y.; Feng, J.; Jia, Q.; Song, Q.; Zhu, B.; et al. Immune Phenotyping Based on the Neutrophil-to-Lymphocyte Ratio and IgG Level Predicts Disease Severity and Outcome for Patients With COVID-19. *Front. Mol. Biosci.* **2020**, *7*, 157. [[CrossRef](#)]
22. Passlick, B.; Flieger, D.; Ziegler-Heitbrock, H.W.L. Identification and Characterization of a Novel Monocyte Subpopulation in Human Peripheral Blood. *Blood* **1989**, *74*, 2527–2534. [[CrossRef](#)] [[PubMed](#)]
23. Grage-Griebenow, E.; Zawatzky, R.; Kahlert, H.; Brade, L.; Flad, H.-D.; Ernst, M. Identification of a Novel Dendritic Cell-like Subset of CD64+/CD16+ Blood Monocytes. *Eur. J. Immunol.* **2001**, *31*, 48–56. [[CrossRef](#)]
24. Ziegler-Heitbrock, L.; Ancuta, P.; Crowe, S.; Dalod, M.; Grau, V.; Hart, D.N.; Leenen, P.J.M.; Liu, Y.-J.; MacPherson, G.; Randolph, G.J.; et al. Nomenclature of Monocytes and Dendritic Cells in Blood. *Blood* **2010**, *116*, e74–e80. [[CrossRef](#)] [[PubMed](#)]
25. Zawada, A.M.; Rogacev, K.S.; Rotter, B.; Winter, P.; Marell, R.-R.; Fliser, D.; Heine, G.H. SuperSAGE Evidence for CD14++CD16+ Monocytes as a Third Monocyte Subset. *Blood* **2011**, *118*, e50–e61. [[CrossRef](#)]
26. Wong, K.L.; Tai, J.J.-Y.; Wong, W.-C.; Han, H.; Sem, X.; Yeap, W.-H.; Kourilsky, P.; Wong, S.-C. Gene Expression Profiling Reveals the Defining Features of the Classical, Intermediate, and Nonclassical Human Monocyte Subsets. *Blood* **2011**, *118*, e16–e31. [[CrossRef](#)]
27. Gren, S.T.; Rasmussen, T.B.; Janciauskiene, S.; Håkansson, K.; Gerwien, J.G.; Grip, O. A Single-Cell Gene-Expression Profile Reveals Inter-Cellular Heterogeneity within Human Monocyte Subsets. *PLoS ONE* **2015**, *10*, e0144351. [[CrossRef](#)]
28. Schulte-Schrepping, J.; Reusch, N.; Paclik, D.; Baßler, K.; Schlickeiser, S.; Zhang, B.; Krämer, B.; Krammer, T.; Brumhard, S.; Bonaguro, L.; et al. Severe COVID-19 Is Marked by a Dysregulated Myeloid Cell Compartment. *Cell* **2020**, *182*, 1419–1440.e23. [[CrossRef](#)]
29. Knaus, W.A.; Draper, E.A.; Wagner, D.P.; Zimmerman, J.E. APACHE II: A Severity of Disease Classification System. *Crit. Care Med.* **1985**, *13*, 818–829. [[CrossRef](#)]
30. Matthay, M.A.; Ware, L.B.; Zimmerman, G.A. The Acute Respiratory Distress Syndrome. *J. Clin. Investig.* **2012**, *122*, 2731–2740. [[CrossRef](#)]
31. Horovitz, J.H.; Carrico, C.J.; Shires, G.T. Pulmonary Response to Major Injury. *Arch. Surg.* **1974**, *108*, 349–355. [[CrossRef](#)]
32. Silvin, A.; Chapuis, N.; Dunsmore, G.; Goubet, A.-G.; Dubuisson, A.; Derosa, L.; Almire, C.; Hénon, C.; Kosmider, O.; Droin, N.; et al. Elevated Calprotectin and Abnormal Myeloid Cell Subsets Discriminate Severe from Mild COVID-19. *Cell* **2020**, *182*, 1401–1418.e18. [[CrossRef](#)] [[PubMed](#)]
33. Zhou, Y.; Fu, B.; Zheng, X.; Wang, D.; Zhao, C.; Qi, Y.; Sun, R.; Tian, Z.; Xu, X.; Wei, H. Pathogenic T-Cells and Inflammatory Monocytes Incite Inflammatory Storms in Severe COVID-19 Patients. *Natl. Sci. Rev.* **2020**, *7*, 998–1002. [[CrossRef](#)] [[PubMed](#)]
34. Patterson, B.K.; Francisco, E.B.; Yogendra, R.; Long, E.; Pise, A.; Rodrigues, H.; Hall, E.; Herrera, M.; Parikh, P.; Guevara-Coto, J.; et al. Persistence of SARS CoV-2 S1 Protein in CD16+ Monocytes in Post-Acute Sequelae of COVID-19 (PASC) up to 15 Months Post-Infection. *Front. Immunol.* **2022**, *12*, 5526. [[CrossRef](#)]
35. Mairpady Shambat, S.; Gómez-Mejía, A.; Schweizer, T.A.; Huemer, M.; Chang, C.-C.; Acevedo, C.; Bergada-Pijuan, J.; Vulin, C.; Hofmaenner, D.A.; Scheier, T.C.; et al. Hyperinflammatory Environment Drives Dysfunctional Myeloid Cell Effector Response to Bacterial Challenge in COVID-19. *PLoS Pathog.* **2022**, *18*, e1010176. [[CrossRef](#)] [[PubMed](#)]
36. Karawajczyk, M.; Douhan Håkansson, L.; Lipcsey, M.; Hultström, M.; Pauksens, K.; Frithiof, R.; Larsson, A. High Expression of Neutrophil and Monocyte CD64 with Simultaneous Lack of Upregulation of Adhesion Receptors CD11b, CD162, CD15, CD65 on Neutrophils in Severe COVID-19. *Ther. Adv. Infect.* **2021**, *8*, 20499361211034064. [[CrossRef](#)] [[PubMed](#)]

37. Ivetic, A.; Hoskins Green, H.L.; Hart, S.J. L-Selectin: A Major Regulator of Leukocyte Adhesion, Migration and Signaling. *Front. Immunol.* **2019**, *10*, 1068. [CrossRef] [PubMed]
38. Lee, D.; Schultz, J.B.; Knauf, P.A.; King, M.R. Mechanical Shedding of L-Selectin from the Neutrophil Surface during Rolling on Sialyl Lewis x under Flow. *J. Biol. Chem.* **2007**, *282*, 4812–4820. [CrossRef]
39. Jin, Y.; Ji, W.; Yang, H.; Chen, S.; Zhang, W.; Duan, G. Endothelial Activation and Dysfunction in COVID-19: From Basic Mechanisms to Potential Therapeutic Approaches. *Sig. Transduct. Target. Ther.* **2020**, *5*, 293. [CrossRef]
40. Middleton, E.A.; He, X.-Y.; Denorme, F.; Campbell, R.A.; Ng, D.; Salvatore, S.P.; Mostyka, M.; Baxter-Stoltzfus, A.; Borczuk, A.C.; Loda, M.; et al. Neutrophil Extracellular Traps Contribute to Immunothrombosis in COVID-19 Acute Respiratory Distress Syndrome. *Blood* **2020**, *136*, 1169–1179. [CrossRef]
41. Riemer, C.; Mack, E.; Burchert, A.; Gündisch, M.; Greib, S.; Etati, R.; Tarawneh, T.; Karim, I.; Keller, C.; Renz, H.; et al. Dysgranulopoiesis in Patients with Coronavirus Disease 2019. *Acta Haematol. Pol.* **2021**, *52*, 6. [CrossRef]
42. Lacy, P. Mechanisms of Degranulation in Neutrophils. *Allergy Asthma Clin. Immunol.* **2006**, *2*, 98. [CrossRef]
43. Tosi, M.F.; Zakem, H. Surface Expression of Fc Gamma Receptor III (CD16) on Chemoattractant-Stimulated Neutrophils Is Determined by Both Surface Shedding and Translocation from Intracellular Storage Compartments. *J. Clin. Investig.* **1992**, *90*, 462–470. [CrossRef] [PubMed]
44. Huizinga, T.W.; de Haas, M.; Kleijer, M.; Nuijens, J.H.; Roos, D.; von dem Borne, A.E. Soluble Fc Gamma Receptor III in Human Plasma Originates from Release by Neutrophils. *J. Clin. Investig.* **1990**, *86*, 416–423. [CrossRef] [PubMed]
45. Middelhoven, P.J.; Buul, J.D.V.; Hordijk, P.L.; Roos, D. Different Proteolytic Mechanisms Involved in FcγRIIIb Shedding from Human Neutrophils. *Clin. Exp. Immunol.* **2001**, *125*, 169–175. [CrossRef] [PubMed]
46. Perussia, B.; Dayton, E.T.; Lazarus, R.; Fanning, V.; Trinchieri, G. Immune Interferon Induces the Receptor for Monomeric IgG1 on Human Monocytic and Myeloid Cells. *J. Exp. Med.* **1983**, *158*, 1092–1113. [CrossRef]
47. Repp, R.; Valerius, T.; Sendler, A.; Gramatzki, M.; Iro, H.; Kalden, J.; Platzer, E. Neutrophils Express the High Affinity Receptor for IgG (Fc Gamma RI, CD64) after in Vivo Application of Recombinant Human Granulocyte Colony-Stimulating Factor. *Blood* **1991**, *78*, 885–889. [CrossRef]
48. Zhang, Y.; Boesen, C.C.; Radaev, S.; Brooks, A.G.; Fridman, W.-H.; Sautes-Fridman, C.; Sun, P.D. Crystal Structure of the Extracellular Domain of a Human FcγRIII. *Immunity* **2000**, *13*, 387–395. [CrossRef]
49. Kimberly, R.; Ahlstrom, J.; Click, M.; Edberg, J. The Glycosyl Phosphatidylinositol-Linked FcγRIII(PMN) Mediates Transmembrane Signaling Events Distinct from FcγRII. *J. Exp. Med.* **1990**, *171*, 1239–1255. [CrossRef]
50. Unkeless, J.C.; Shen, Z.; Lin, C.-W.; DeBeus, E. Function of Human FcγRIIA and FcγRIIIB. *Semin. Immunol.* **1995**, *7*, 37–44. [CrossRef]
51. Ankerhold, J.; Giese, S.; Kolb, P.; Maul-Pavicic, A.; Voll, R.E.; Göppert, N.; Ciminski, K.; Kreutz, C.; Lothar, A.; Salzer, U.; et al. Circulating Multimeric Immune Complexes Drive Immunopathology in COVID-19. 2021. Available online: <https://www.biorxiv.org/content/10.1101/2021.06.25.449893v4> (accessed on 2 July 2022). [CrossRef]
52. Davis, B.H.; Olsen, S.H.; Ahmad, E.; Bigelow, N.C. Neutrophil CD64 Is an Improved Indicator of Infection or Sepsis in Emergency Department Patients. *Arch. Pathol. Lab. Med.* **2006**, *130*, 654–661. [CrossRef]
53. Muller Kobold, A.C.; Tulleken, J.E.; Zijlstra, J.G.; Sluiter, W.; Hermans, J.; Kallenberg, C.G.; Tervaert, J.W. Leukocyte Activation in Sepsis; Correlations with Disease State and Mortality. *Intensive Care Med.* **2000**, *26*, 883–892. [CrossRef]
54. Cid, J.; García-Pardo, G.; Aguinaco, R.; Sánchez, R.; Llorente, A. Neutrophil CD64: Diagnostic Accuracy and Prognostic Value in Patients Presenting to the Emergency Department. *Eur. J. Clin. Microbiol. Infect. Dis* **2011**, *30*, 845–852. [CrossRef] [PubMed]
55. Song, S.H.; Kim, H.K.; Park, M.H.; Cho, H.-I. Neutrophil CD64 Expression Is Associated with Severity and Prognosis of Disseminated Intravascular Coagulation. *Thromb. Res.* **2008**, *121*, 499–507. [CrossRef] [PubMed]
56. Bradley, P.; Frost, F.; Tharmaratnam, K.; Wootton, D.G. Utility of Established Prognostic Scores in COVID-19 Hospital Admissions: Multicentre Prospective Evaluation of CURB-65, NEWS2 and QSOFA. *BMJ Open Resp. Res.* **2020**, *7*, e000729. [CrossRef] [PubMed]
57. Bradley, J.; Sbaih, N.; Chandler, T.R.; Furmanek, S.; Ramirez, J.A.; Cavallazzi, R. Pneumonia Severity Index and CURB-65 Score Are Good Predictors of Mortality in Hospitalized Patients With SARS-CoV-2 Community-Acquired Pneumonia. *Chest* **2022**, *161*, 927–936. [CrossRef]
58. Artero, A.; Madrazo, M.; Fernández-Garcés, M.; Muiño Miguez, A.; González García, A.; Crestelo Vieitez, A.; García Guijarro, E.; Fonseca Aizpuru, E.M.; García Gómez, M.; Areses Manrique, M.; et al. Severity Scores in COVID-19 Pneumonia: A Multicenter, Retrospective, Cohort Study. *J. Gen. Intern. Med.* **2021**, *36*, 1338–1345. [CrossRef]